

INTERNATIONAL SOCIETY FOR SOIL MECHANICS AND GEOTECHNICAL ENGINEERING



This paper was downloaded from the Online Library of the International Society for Soil Mechanics and Geotechnical Engineering (ISSMGE). The library is available here:

<https://www.issmge.org/publications/online-library>

This is an open-access database that archives thousands of papers published under the Auspices of the ISSMGE and maintained by the Innovation and Development Committee of ISSMGE.

SIMULATION OF SOIL-PILE-STRUCTURE INTERACTION THROUGH MULTI-DIMENSIONAL SHAKING TABLE TESTS USING E-DEFENSE FACILITY

Youhao ZHOU¹, Hiroyuki YOSHIDA², Hiroko SUZUKI³, Yasushi NUKUI⁴, Kohji TOKIMATSU⁵

ABSTRACT

In order to examine the applicability of the three-dimensional finite element method for evaluating pile foundation behavior while soil shows strong nonlinearity, numerical simulations of two soil-pile-structure models subjected to strong shaking were performed. The tests were conducted using the large-scale shaking table at the E-Defense to investigate the response and failure of a nearly full-scale pile-structure system under multi-dimensional loading. It has been shown that the numerical analysis can reproduce the behaviors of the piles and superstructure as well as those of soil with a reasonable degree of accuracy, suggesting its applicability to soil-pile-structure system subjected to strong 3-D shaking. The comparison of the two analytical results further indicates that the pile head rigidity might have decreased prior to the later test discussed in this paper.

Keywords: Shaking Table Test, E-Defense, Finite Element Method, Non-Linear Analysis, Pile

INTRODUCTION

Most of Japanese metropolises lie on soft ground near seas and large rivers. For this reason, pile foundations are commonly applied for substructures, representing 70~80% of all buildings. Pile foundation is, however, weak in horizontal direction, thus soil and structures tend to be damaged by both inertial force from superstructures and kinematic force from ground displacement during earthquakes with large-scale horizontal shaking. Despite of this fact, mechanism of those damages is, due to the lack of data since no observation has ever been made, not fully understood.

In order to gain sufficient data to establish a design method for pile foundation with failure of piles taken into account, a series of shaking table tests using soil-pile-structure models was performed (MEXT and NIED, 2006; Suzuki et al., 2008; Tokimatsu et al., 2008). The E-Defense shaking table platform and a cylindrical laminar shear box were used for the tests, and a full-scale pile-structure system was subjected to a series of single- or multi-dimensional loading. In cases where large scale loading was applied, subsidence and residual displacement of footing were observed, and data including pile damage process were obtained.

¹ Master Student, Dept. Architecture and Building Engineering, Tokyo Institute of Technology, Japan

² Chief, Arch. & Struct. Eng. Operation Center, Tokyo Electric Power Services Co., Ltd., Japan (TITECH)

³ Assistant Professor, Dept. Architecture and Building Engineering, Tokyo Institute of Technology, Japan

⁴ Group Manager, R&D Center, Tokyo Electric Power Company, Japan

⁵ Professor, Dept. Architecture and Building Engineering, Tokyo Institute of Technology, Japan

By performing numerical analysis of abovementioned shaking table tests using three-dimensional finite element method, this paper verifies the validity of the evaluation method on dynamical behavior of pile foundation structures when soil shows strong nonlinearity.

SHAKING TABLE TESTS

The E-Defense shaking table platform has a dimension of 15 m long and 20 m wide. Figure 1 and Photo 1 show a test model constructed in a cylindrical laminar box 6.5 m high with an outside diameter of 8.0 m. It consists of forty-one stacked ring flanges, enabling two-dimensional shear deformation of the inside soil.

A 3x3 steel pile group was used for the test. The piles were labeled A1 to C3 according to their locations within the pile group, as shown in Figure 1. Each pile had a diameter of 152.4 mm and a wall thickness of 2.0 mm. The piles were set up with a horizontal space of four-pile diameters center to center. Their tips were jointed to the laminar box base with pins and their heads were fixed to the footing of a weight of 10 tons.

Dry Albany sand from Australia was used for preparing the sand deposit. Figure 2 shows the grain size distribution of the sand. The sand had a mean grain size D_{50} of 0.31 mm and a coefficient of uniformity U_c of 2.0. After setting a pile group in the laminar box, the dry sand was air-pluviated and compacted at every 0.275m to a relative density of about 70% to form a uniform sand deposit with a thickness of 6.3m.

As listed in Table 1, a total of five test series named A to E was conducted in alphabetical order, in which the presence of foundation embedment and superstructure, and the natural period of superstructure, as well as the type of input motions, and their component and maximum accelerations were varied. In test series C and E, which this paper focuses on, natural frequencies of the soil which was obtained from microtremor observation, were about 7.0 Hz and 7.9 Hz, respectively. Natural frequency of the superstructure in series E was about 6.0 Hz.

Table 2 shows the list of shaking conditions of test series. In order to clarify the effect of natural period of superstructure on dynamic behavior of test model, the tests were conducted under one-, two- or three-dimensional shaking with three types of

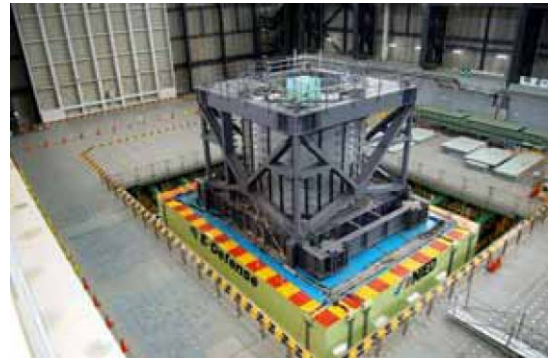


Photo 1 Test Model on Large Shaking Table

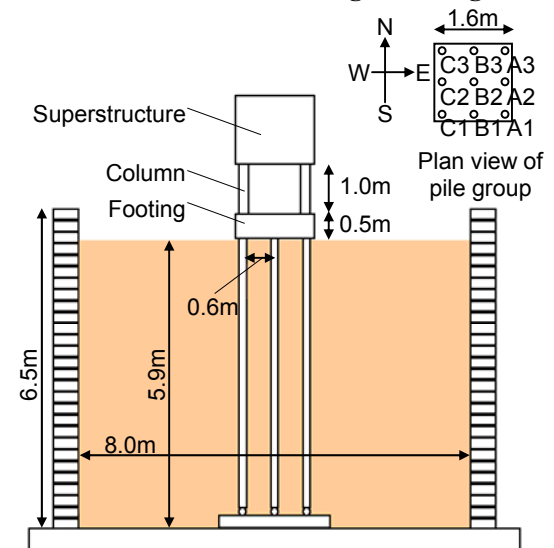


Figure 1. Soil-Pile-Structure Model (Series E)

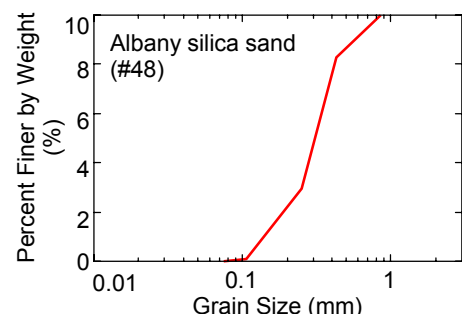


Figure 2. Grain Size Distribution of Albany Sand

Table 1. Test Model Series

	Superstructure	Embedment
A	Rigid (Ultra-short period)	Yes
B	Long period	Yes
C	No	Yes
D	Short period	Yes
E	Short period	No

Table 2. Shaking Conditions of Test Series

	Maximum input acceleration (cm/s ²)			
	JR Takatori		Taft and Tottori	
	XYZ	XY, X, Y	XYZ	XY, X, Y
A, B	30, 90		30, 90	-
C	30, 90, <u>110</u>		30, 90, 110	-
D	30, 90		30, 90	
E	30, 90 <u>110</u> 300, 600	30, 90	30, 90 (Taft only)	-

ground motions, which dominate in different period ranges, with maximum horizontal accelerations adjusted to 30 cm/s² and 90 cm/s² (and 110 cm/s² in selected cases). Pile strains were within elastic range in all test series. In addition, in order to investigate the pile destruction process induced by ground motion, additional tests were conducted for series E, under three-dimensional shaking with maximum accelerations at levels in actual earthquakes. JR Takatori wave was used, with maximum horizontal accelerations at 300 cm/s² and 600 cm/s².

Among the cases conducted with three-dimensional JR Takatori wave, this paper focuses on the ones in test series C and E with maximum acceleration adjusted to 110 cm/s² (as underlined in Table 2), in which the soil showed strong nonlinearity, and reports the results of numerical analysis.

NUMERICAL ANALYSIS

Analytical Model

Numerical analyses were conducted with a three-dimensional FEM model using analysis code EENA3D developed by TEPCO (Yoshida et al., 2006; Yoshida et al., 2008). Figure 3 and Figure 4 illustrate the analytical model.

The laminar shear box is modeled as solid elements with equivalent mass and adequately small stiffness. Degree of freedom is restrained, so that each ring frame of the shear box may maintain its plane during shear deformation. To take the effect of rocking behavior of the shaking table into account, vertical springs are placed at eight points at bottom of the box.

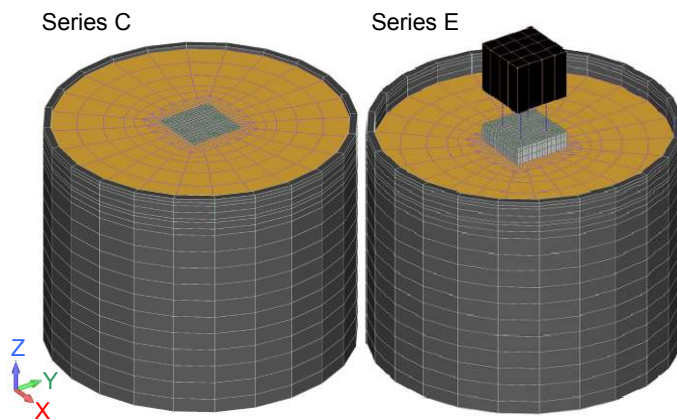


Figure 3. Analysis Model (Overview)

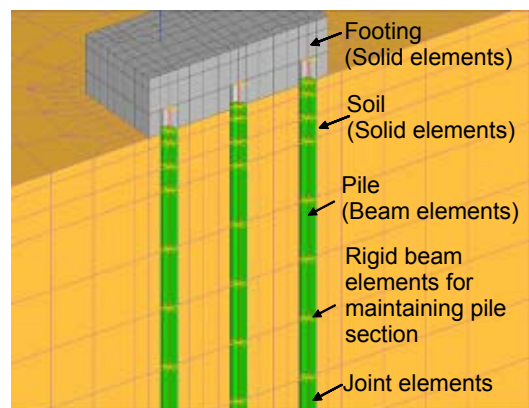


Figure 4. Details on Pile and Footing

In the test model, steel pipe piles and steel footing were rigidly fixed together by injecting non-shrinkage cement into gaps between them. However, it is possible that the cement had been broken during the tests, and rigidity at pile heads had decreased. In order to simulate the possible fracturing of cement and the decreasing of pile head rigidity, and to investigate the effect of pile head rigidity on the dynamic behavior of piles, two models are made for each case. Figure 5 compares the differences between the two models. In model 1, the footing bottom and the pile head are fixed together, while in model 2, the connections between the footing bottom and the pile head are partially removed. A static loading analysis is performed to investigate the pile head rigidity, and the results are 0.96 in model 1 and 0.86 in model 2, respectively.

Specifications and dynamic strain dependency of the soil are explained in Table 3 and Figure 6, respectively. Velocities of P and S waves, V_P and V_S , are obtained by performing regression analysis on results of PS logging depending on overburden pressure σ'_z . Poisson's ratio ν is calculated from V_P and V_S . As explained in Figure 7, in order not to include engineering judgments in parameter setting, discrete data of G/G_0 - γ regression curve shown in Figure 6 are directly inputted to simulate soil's nonlinearity. τ - γ relation is obtained from inputted G/G_0 - γ dynamic strain dependency curve, also as discrete data. The discrete τ - γ relation is linearly interpolated to define skeleton curve. Cohesion c is set to zero. Internal friction angle ϕ is obtained from Equation 1;

$$\tau_{max} = \sigma_c \cdot \tan \phi \quad (1)$$

where σ_c is consolidation stress; and shear strength τ_{max} is defined by the maximum value of τ - γ skeleton curve. Obtained internal friction angle is used to define the strength of joint elements.

In addition, in this study, the nonlinear model of soil concerning its shear deformation component is defined by the second constant J_2 of deviatoric stress q , based on von Mises' failure criterion. Relation of equivalent stress $\sigma_e (= \sqrt{1/2 \times s_{ij} s_{ij}})$ and equivalent strain $e (= \sqrt{2 \times \varepsilon_{ij} \varepsilon_{ij}})$, which are expressed by root of deviatoric stress q and deviatoric strain ε_s respectively, is defined by stress-strain relation given by Equation 2.

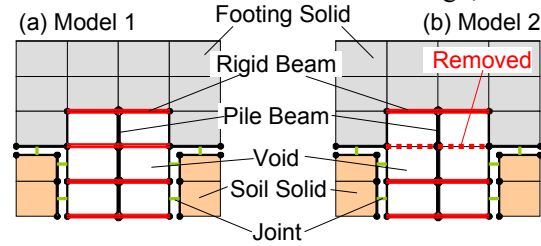


Figure 5. Modification of Pile Head Rigidity

Table 3. Specification of Soil

Parameter	Value
Density ρ (t/m ³)	1.709
S wave velocity V_S (m/s)	$86\sigma_v^{0.25}$
P wave velocity V_P (m/s)	$146\sigma_v^{0.25}$
Poisson's ratio ν	0.234
Cohesion c (kPa)	0
Internal friction ϕ (°)	29.5

* σ_v : Overburden pressure (kN/m²)

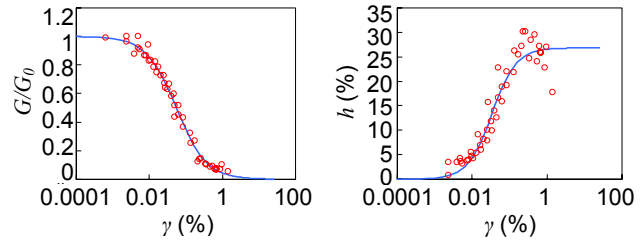


Figure 6. G/G_0 - γ , h - γ Relation

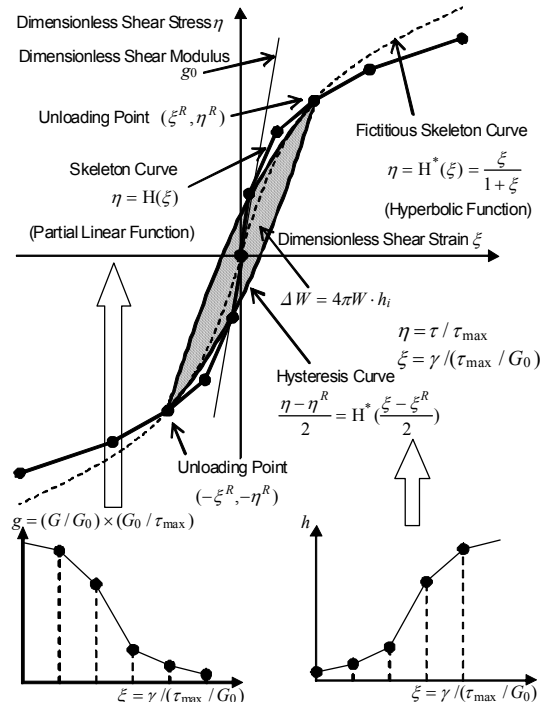


Figure 7. Modeling of Nonlinearity for Shear Strain

$$\sigma_e = G \cdot e \quad (2)$$

Dynamic strain dependencies ($G/G_0-\gamma$, $h-\gamma$) are considered in Equation 2. However, since equivalent stress σ_e and equivalent strain e both only take positive values, it is impossible to identify whether it is pulsating or alternating. In order to draw hysteresis curve, the radius of yield surface in π plain is given as deviatoric strain e (Yoshida et al., 1993).

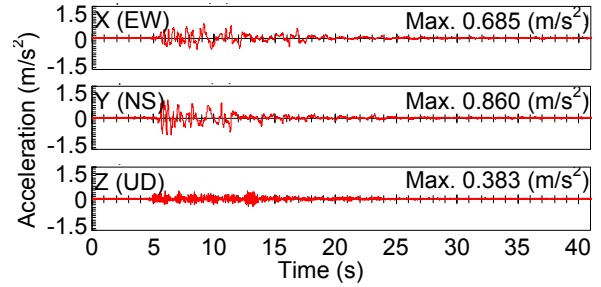


Figure 8. Input Motion

Input motion, as shown in Figure 8, is calculated by averaging each component of four observed records obtained at bottom of the shear box. All three components of the input motion are applied simultaneously to the bottom center of the box.

Numerical Analysis Results

Figures 9 and 10 show distributions of maximum acceleration in pile, footing, superstructure and soil. The Z components of pile accelerations are missing because no observation was made for vertical behavior of the piles. In series C the observed maximum acceleration takes its peak value at the footing, while in series

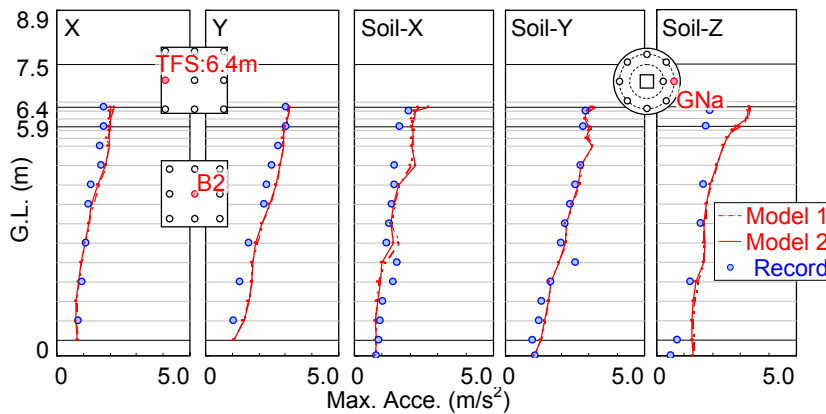


Figure 9. Maximum Acceleration Distribution (Series C)

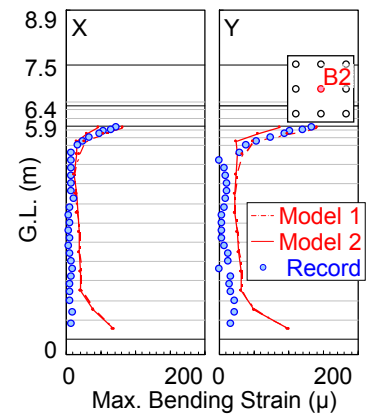


Figure 11. Maximum Pile Strain Distribution (Series C)

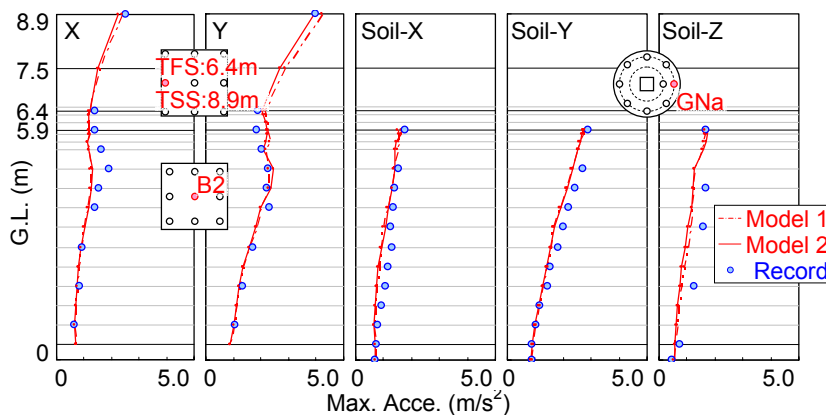


Figure 10. Maximum Acceleration Distribution (Series E)

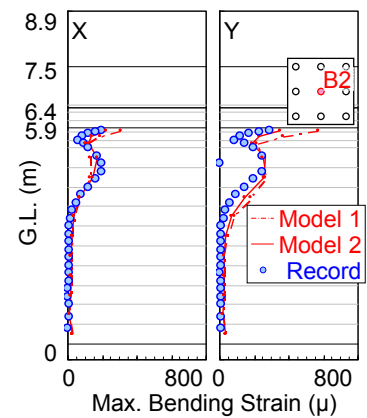


Figure 12. Maximum Pile Strain Distribution (Series E)

E the acceleration at footing is smaller than that of underground. This is because the second mode of response in series E is relatively large, due to the presence of the superstructure. Vertical acceleration of soil near the surface is overestimated in series C, which is a result of analytical noise. The estimated results reproduce the observed accelerations in soil, pile and superstructure fairly well, indicating the validity of the three-dimensional nonlinear analysis model. Notably, there is no significant difference between the results from model 1 and 2, which indicates that the pile head rigidity does not affect the response of soil, pile or superstructure.

Figures 11 and 12 show the distribution of maximum bending strain of pile. Strains at the pile tips are overestimated in both series. This indicates that, although soil is considered to exist around the pile tips in the analysis model, rigidity of the pile tips was lower in the actual test models. In series C, as shown in Figure 11, the observed bending strain level is low and becomes higher only near the pile head, since the inertial force is small. The estimated result from model 1 is in good agreement in all depths with the observed data, while the result from model 2 tends to underestimate the strain at the pile head. On the other hand, in series E, as shown in Figure 12, the observed strain level is high due to the large inertial force, and has a peak underground as well as near pile head. The estimated result from model 1 overestimates the strain at the pile head, while the result from model 2 is in good agreement with the observed one in all depths. This suggests that the pile head rigidity might have decreased in a test case conducted after series C and prior to series E.

Acceleration time histories in both series are shown in Figures 13-16. Regardless of pile head rigidity, estimated accelerations are in good agreement with observed ones, reproducing the observed waveforms as well as their peak values, not only in Y direction which is the strong axis of the seismic wave, but also in X direction which is the weak axis. Accelerations in vertical direction are also reproduced with a

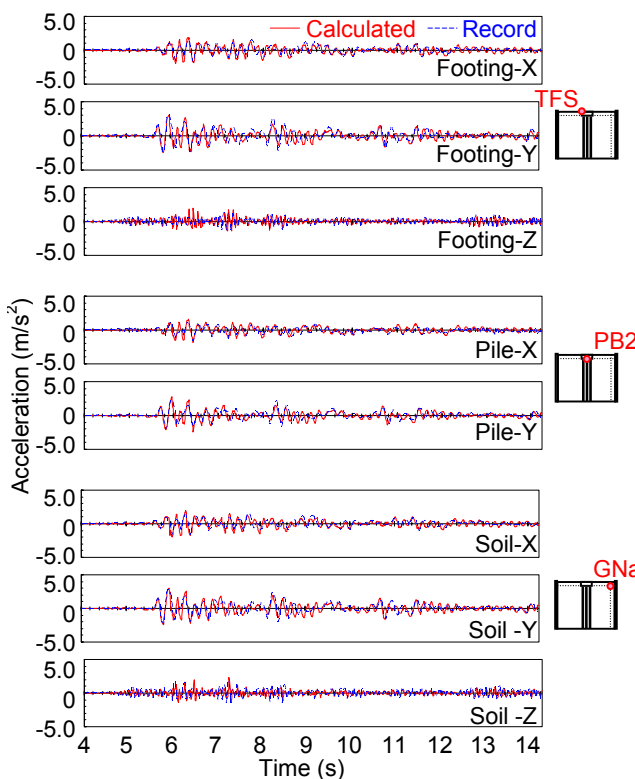


Figure 13. Acceleration Time Histories (Series C, Model 1)

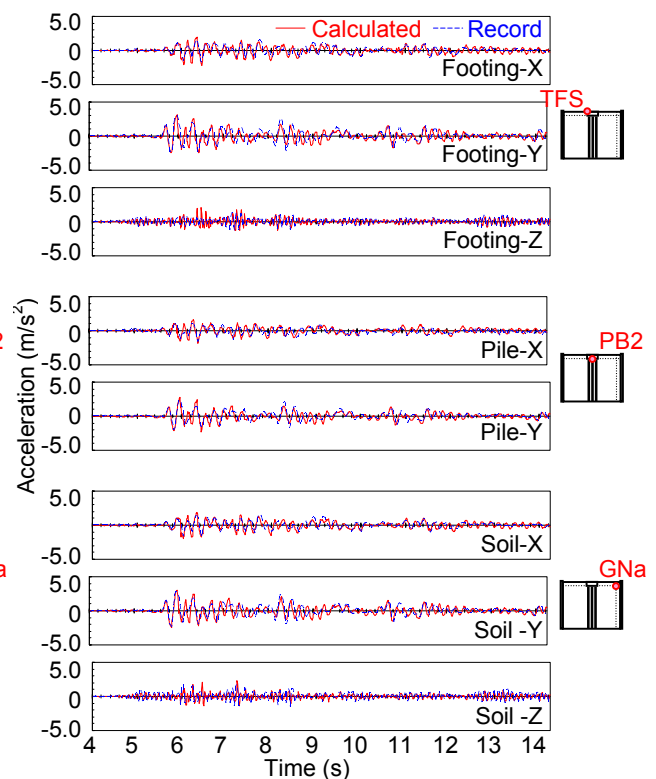


Figure 14. Acceleration Time Histories (Series C, Model 2)

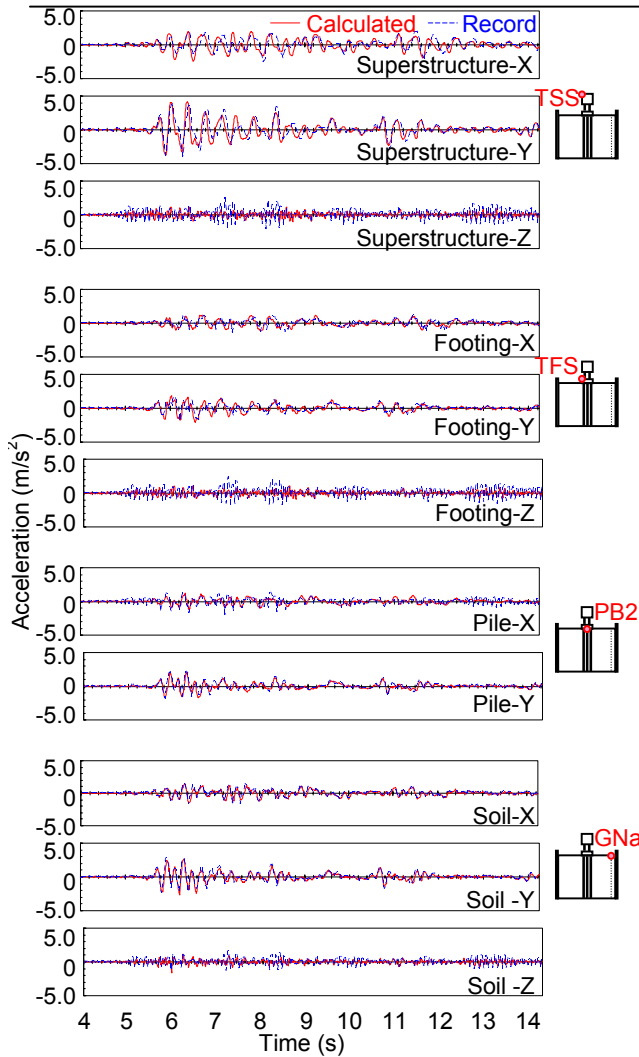


Figure 15. Acceleration Time Histories
(Series E, Model 1)

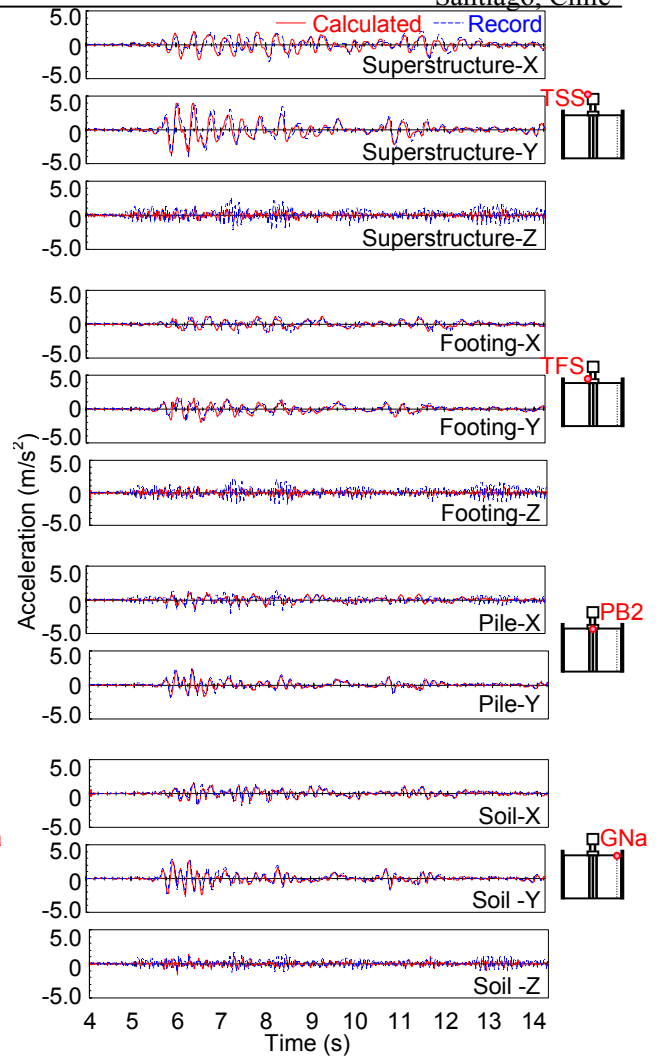


Figure 16. Acceleration Time Histories
(Series E, Model 2)

reasonable degree of accuracy, although some noise can be seen. It therefore suggests that, for the overall behavior, the obtained response is appropriate.

Time histories of bending strain are shown in Figures 17-20. In series C which is shown in Figures 17 and 18, the estimated results from model 1 have a better agreement with observed ones, while in series E which is shown in Figures 19 and 20, the estimated results from model 2 have a better agreement with observed ones. This again suggests a decrease in the pile head rigidity during the shaking table tests.

Overall, it can be confirmed that the estimated results from both series are able to reproduce the behaviors of the test models, regardless of the presence of the superstructure or the embedment of the footing.

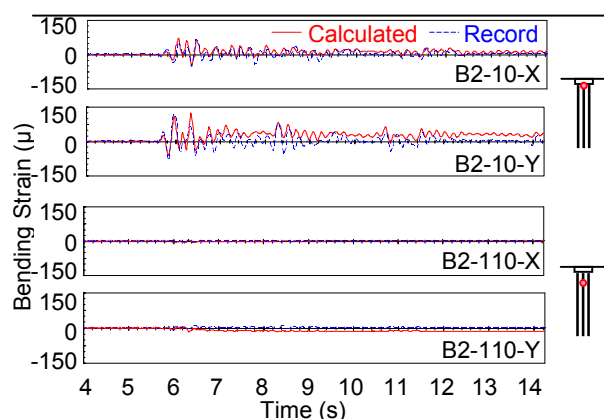


Figure 17. Bending Strains Time Histories (Series C, Model 1)

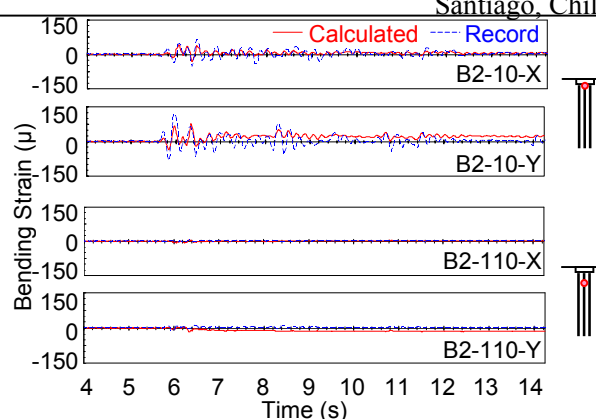


Figure 18. Bending Strains Time Histories (Series C, Model 2)

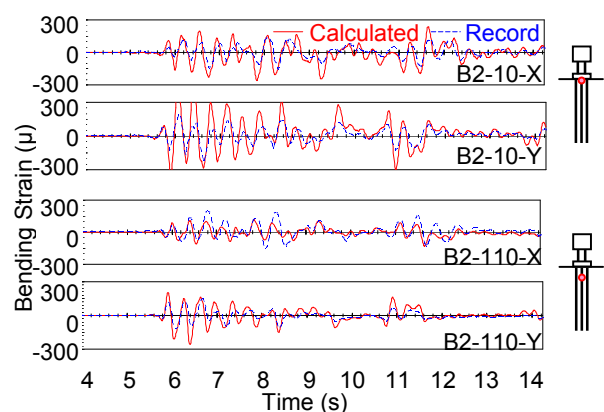


Figure 19. Bending Strains Time Histories (Series E, Model 1)

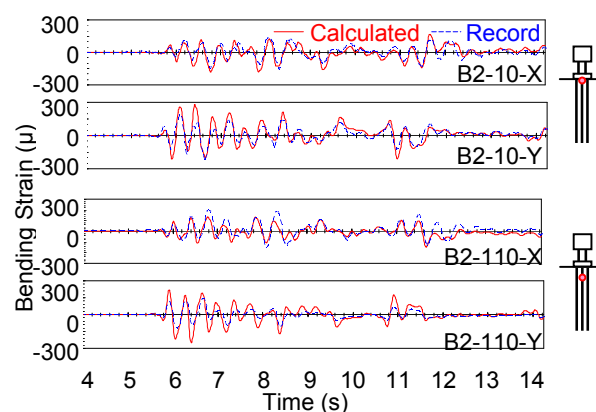


Figure 20. Bending Strains Time Histories (Series E, Model 2)

CONCLUSIONS

In order to confirm the applicability of the three-dimensional finite element method for evaluating pile foundation behavior while soil shows strong nonlinearity, numerical simulation of two soil-pile-structure models subjected to strong shaking were performed. The tests were conducted using the large-scale shaking table at the E-Defense. It has been shown that the numerical analysis can reproduce the behaviors of the piles and superstructure as well as those of soil with a reasonable degree of accuracy, suggesting its applicability to soil-pile-structure system subjected to strong 3-D shaking. The comparison of the two analytical results further indicates that the pile head rigidity might have decreased prior to the later test discussed in this paper.

ACKNOWLEDGMENTS

The study described herein was made possible through Special Project for Earthquake Disaster Mitigation in Urban Areas, supported by the Ministry of Education, Culture, Sports, Science and Technology (MEXT). The authors express their sincere thanks to the above organization.

REFERENCES

- MEXT and NIED (2006), Research Theme No. 2 Annual Report of the fiscal year 2005, Special project for earthquake disaster mitigation in urban area, 831p (in Japanese).
- H. Suzuki, K. Tokimatsu, M. Sato and K. Tabata (2008), "Stress distribution within pile group during failure process in large shaking table tests", *Proc. of 39th Japan National Conference on Geotechnical Engineering*, pp. 1161-1162 (in Japanese).
- K. Tokimatsu, H. Suzuki, K. Tabata and M. Sato (2007), "Three-dimensional shaking table tests on soil-pile structure models using E-Defense facility," *Proc. of 4th International Conference on Earthquake Geotechnical Engineering*, 11 pp.
- H. Yoshida, K. Tokimatsu, T. Sugiyama and T. Shiomi (2008), "Practical Three- Dimensional Effective Stress Analysis Considering Cyclic Mobility Behavior," *Proc. of 14th World Conference on Earthquake Engineering*, Paper_ID 04-01-0061.
- H. Yoshida, T. Ishida, T. Shiomi, K. Hijikata, F. Yanagishita, T. Sugiyama, Y. Ohmiya and K. Tokimatsu et al. (2006) "Study on Practicable 3-Dimensional Effective Stress Analysis Using the Ground Survey Result", *Summaries of technical papers of Annual Meeting AIJ*, p623-626, B-1 (in Japanese).
- N. Yoshida and S. Tsujino (1993), "A Simplified Practical Stress-Strain Model for the Multi-Dimensional Analysis under Repeated Loading Part2 Consideration of Dilatancy", *Proc. of Annual Conference of the Japan Society of Civil Engineers*, pp.1221-1224 (in Japanese).